Thin Film Elastic Modulus of Degradable Tyrosine-Derived Polycarbonate Biomaterials and Their Blends

Khaled A. Aamer,*,† Christopher M. Stafford,† Lee J. Richter,‡ Joachim Kohn,§ and Matthew L. Becker*,†

Polymers Division and Surface and Microanalysis Science Division, National Institute of Standards and Technology, 100 Bureau Drive, Gaithersburg, Maryland 20899-854, and New Jersey Center for Biomaterials, Rutgers University, Piscataway, New Jersey 08854

Received September 17, 2008; Revised Manuscript Received December 10, 2008

ABSTRACT: The integrity, function, and performance of biomedical devices having thin polymeric coatings are critically dependent on the mechanical properties of the film, including the elastic modulus. In this report, the elastic moduli of several tyrosine-derived polycarbonate thin films, specifically desaminotyrosyl ethyl tyrosine polycarbonates p(DTE carbonate), an iodinated derivative p(I_2-DTE carbonate), and several discrete blends are measured using a method based on surface wrinkling. The data shows that the elastic modulus does not vary significantly with the blend composition as the weight percentage of p(I_2-DTE carbonate) increases for films of uniform thickness in the range of 67 to 200 nm. As a function of film thickness, the observed elastic moduli of p(DTE carbonate), p(I_2-DTE carbonate) and their 50:50 by mass blend show little variation over the range 30 to 200 nm.

Introduction

Tyrosine-derived polycarbonates are a novel class of biodegradable polymers that are used in biomaterials applications.[1−3] The materials share a structurally identical backbone with a rich chemical and structural diversity present in the pendent ester substituent. Recent advances in copolymerization with polyethylene glycol and other monomers have served to further increase the chemical diversity of the library.[4−6] These structural changes affect significantly the mechanical properties, degradation rates, and subsequent cellular responses of the respective polymers. Several derivatives have entered clinical trials with promising early results, including the recent U.S. Food and Drug Administration approval of a single component material used for hernia mesh.[7] Additional applications such as deployable cardiovascular stents, tissue engineering scaffolds, nanospheres for drug delivery and thin film coatings are under investigation where the stability and mechanical performance of the respective materials are important.[2,3,8−11] In general, the polymers are amorphous and have very low X-ray contrast making visualization by common clinical imaging systems difficult. To increase the radiopacity and enable use of these materials in applications where *in vitro* and *in vivo* imaging is required, including microcomputed tomography (μCT), iodine atoms were incorporated into the aromatic tyrosine monomer subunit.[12,13] Previously, we have found 9% to 46% by mass p(I_2-DTE carbonate) was sufficient for increasing radiopacity depending on the modality used for imaging.[14] However, the incorporation of iodine into polymeric materials often has a distinct influence on the chemical, physical and biological properties, including protein adsorption.[15] Therefore, we have utilized polymer blending as a strategy for increasing radiopacity while minimizing the amount of iodinated material to mitigate significant physical property changes.

Quantitative assessments of the physical and mechanical properties are critical to the efforts to expand these materials into biomedical applications, especially when working in the thin film regime. Several reports have demonstrated that thin film mechanical properties are significantly reduced as the thickness approaches and drops below the end to end distance of individual polymer chains.[16−21] These dramatic losses could potentially lead to device or coating failure or alter significantly the release profiles of incorporated bioactive agents. To probe these effects we examined the influence of composition and film thicknesses on the elastic moduli of the desaminotyrosyl ethyl tyrosine polycarbonates, p(DTE carbonate), the iodinated analogue p(I_2-DTE carbonate), (chemical structures illustrated in Figure 2a), and a series of discrete blends over a range of thicknesses useful in thin film applications using a wrinkling-based technique.

Several wrinkling-based techniques have been developed as metrology platforms to measure the elastic modulus of thin films and coatings.[22,23] These techniques have recently been applied to ultrathin films, soft polymer networks and gels, and even single carbon nanotubes.[22,24,25] In particular, the work by Stafford et al.[22] demonstrated the use of surface wrinkling to

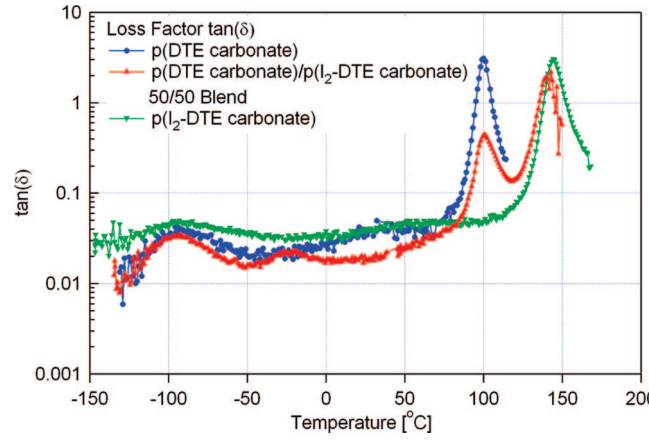

Figure 1. Temperature dependence of the loss tangent (tan (δ)) in dynamic stress relaxation of p(DTE carbonate), p(I_2-DTE carbonate), and their 50:50 mass % blend in the tension mode at a frequency of 1 Hz. Shown are the α-(T_g) and the β-relaxation behavior of both polymers.

* Corresponding authors. E-mail: mlbecker@nist.gov; khaled.aamer@nist.gov.
† Polymers Division, National Institute of Standards and Technology.
‡ Surface and Microanalysis Division, National Institute of Standards and Technology.
§ New Jersey Center for Biomaterials, Rutgers University.

10.1021/ma802115b CCC: $40.75
Published on Web 01/22/2009

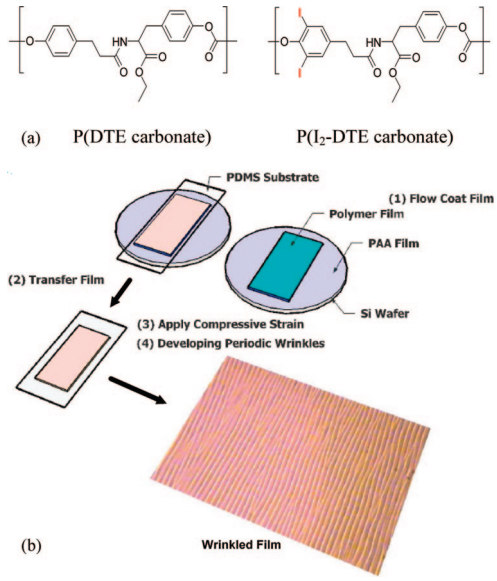

Figure 2. (a) Scheme showing chemical structures of p(DTE carbonate)and p(I_2-DTE carbonate) polymers. (b) Schematic presentation of the steps involved in the SIEBIMM technique.

measure the elastic modulus of a compressed laminate system composed of a stiff thin film on a thick poly(dimethylsiloxane), PDMS, elastic substrate. This wrinkling instability results from an energy mismatch to deform both the thin film and the elastic substrate. The strain energy in the laminate system during compression is minimized by forming highly periodic surface wrinkles with sinusoidal periodicity of critical wavelength.

Mathematically, the critical wavelength, d, is formulated according to eq 1.

$$d = 2\pi h_f \left[\frac{(1-\upsilon_s^2)E_f}{3(1-\upsilon_f^2)E_s}\right]^{1/3} \quad (1)$$

where h_f is thickness of the thin film,υ is the Poisson's ratio, and E is the Young's modulus (subscript f and s denote the thin film and substrate respectively). Rearranging eq 1 yields the thin film's elastic modulus as a function of wrinkling wavelength, film thickness and substrate elastic modulus according to eq 2.

$$E_f = 3\frac{(1-\upsilon_f^2)}{(1-\upsilon_s^2)}\left(\frac{d}{2\pi h_f}\right)^3 E_s \quad (2)$$

As seen in eq 2, the modulus of the thin film depends on the ratio of wrinkling wavelength to film thickness raised to the third power. Therefore, it is critical to have precise and accurate assessments of the buckled wavelength and film thickness.

Experimental Section

Materials. The synthesis and characterization of the desaminotyrosyl ethyl tyrosine polycarbonates, p(DTE carbonate) (mass average molecular mass, M_w = 105 kDa, polydispersity, PDI = 1.76, glass transition temperature, T_g, (differential scanning calorimetry, DSC, bulk) = 100 °C) and p(I_2-DTE carbonate) (M_w = 294 kDa, PDI = 1.86, T_g, (DSC, bulk) = 145 °C), used in this contribution were reported previously.[1,26] 1,4-Dioxane (Sigma-Aldrich), acetone (VWR), chloroform (Sigma-Aldrich), toluene (J. T. Baker), ethanol (Sigma-Aldrich), 1-propanol (Sigma-Aldrich), poly(acrylic acid), poly(dimethylsiloxane) precursors (PDMS, Slygard 184, Dow Chemical Co., Midland, MI), were all used as received. Si wafers ([100], (76.2 ± 0.5) mm diameter, 1 to 20 ohms-cm resistivity, and a thickness of 350 to 400 μm) were obtained from Wafer World, Inc. (West Palm Beach, FL).

PDMS Substrate Preparation. Transparent PDMS substrates were prepared by hand mixing a mixture of the base monomer and a curing agent (10:1, mass ratio). The mixture was vigorously mixed, degassed and cast on a clean sheet of glass 30 × 30 cm^2 on an optical bench. The poured resin was allowed to spread at room temperature, flatten under the effect of gravity forces, release trapped air bubbles, and cure partially under ambient conditions for 24 h. The PDMS was then cured in an oven at 75 °C for 2 h. After cooling to ambient temperature, the PDMS sheet was cut into pieces with dimensions 25 mm × 90 mm to fit the controlled strain stage. The elastic modulus, E_s, of the PDMS substrate used to support thin films was measured using Texture Analyzer (model TA.XT2i, Texture Technologies Corp.) in tension mode. The PDMS substrate had a modulus range between 1.25 × 10^6 Pa and 2.1 × 10^6 Pa as measured by tensile test.

Film Preparation and Transfer. The Si wafers used to support the polymer films were cleaned by rinsing with chloroform, ethanol, toluene and acetone three times each, respectively followed by treatment in an ultraviolet/ozone chamber for 60 min. In order to ease the transfer of the polymer film from the Si wafer into the PDMS substrate, a thin film of poly(acrylic acid) (PAA) was first applied on the Si wafer. A solution of PAA (1.5% by mass in 1-propanol, number average molecular mass, M_n = 2 kDa) was spun coated (157 rad/s for 60 s) on a 7.62 cm Si wafer forming a uniform film thickness of 60 ± 3 nm, unless otherwise stated.

Both uniform and gradient thickness film specimens of p(DTE carbonate), p(I_2-DTE carbonate), and their 75:25, 50:50, 25:75, 10:90% by mass polymer blends were flow coated from polymer solutions, 2% by mass in 1,4-dioxane, on PAA coated Si wafer to form a double layer.[27] Typical flow coating conditions for uniform thickness samples include acceleration of 100 mm/s^2, deceleration of 200 mm/s^2, velocity of 25 mm/s, with a 200 μm gap between the blade and substrate, and a solution volume of 50 μL, unless otherwise stated. Typical flow coating conditions for the gradient thickness films include acceleration of 6 mm/s^2, deceleration of 200 mm/s^2, velocity of 25 mm/s, with a height of 200 μm between the blade and substrate, and solution total volume of 50 μL, unless otherwise stated.

The films were then transferred from Si wafers onto prestretched, 1.5%−2.0% strain, PDMS mounted on a custom-built strain stage by aqueous immersion. The PDMS substrate was carefully attached to the film at an edge and was allowed to wet the PDMS surface from the center outward to prevent trapping air bubbles. The strain stage was flipped upside down and totally immersed in a water bath. The film was allowed to disengage under the action of water diffusion to dissolve the PAA and assisted by the hanging mass of the silicon wafer. After complete transfer of the films to the PDMS surface, the strain stage was lifted from water, the film was washed with water, and air-dried. A compressive strain was applied to the PDMS substrate, and subsequently the film, up to the initiation of surface wrinkles on the surface by the use of an actuator built into the stage. Typically 1.5% to 1.6% compressive strain was sufficient to induce the buckling.

Variable Angle Spectroscopic Ellipsometry (VASE). The thicknesses of the polymer films (including PAA on Si, p(DTR carbonate) film on PAA double layer on Si, and p(DTR carbonate) films on PDMS for uniform and gradient thickness films) were determined by variable angle spectroscopic ellipsometry (VASE) before and after the transfer onto PDMS over the wavelength range of 190 to 1700 nm using a Woollam M-2000-D ellipsometer and vendor supplied software. The reference dielectric function, ε, for PAA was determined by fitting reference films cast on clean, native oxide coated Si wafers. Typically three angles of incidence were used. A simple four phase model (Si, native oxide, film, air) was fit to obtain the dielectric function and thickness of the reference films. The thickness of the native oxide was set by measurements on clean reference wafers. Reference dielectric function for PDMS was determined on stretched, freestanding ≈ 2 mm thick films using VASE. Values of the index of refraction $n = \sqrt{\varepsilon}$ at 633 nm are summarized in Table 1. The value for PDMS is in good agreement with previous Brewster's angle measurements. All reported standard

Table 1. Index of Refraction of Blend Films at 633 nm and the Predicted Values Based on Bruggeman Effective Medium Approximation (EMA) as Well as Film Thickness Prior to and after Film Transfer to Pre-Stretched PDMS

	refractive index (n)		Film Thickness (nm)	
polymer	experimental (±0.002)[a]	EMA	before	after (±4 nm)[a]
p(DTE carbonate)	1.547	1.547	141	149
75% p(DTE carbonate)	1.548	1.555	197	203
50% p(DTE carbonate)	1.561	1.562	184	168
25% p(DTE carbonate)	1.572	1.570	153	142
10% p(DTE carbonate)	1.578	1.575	150	141
p(I_2-DTE carbonate)	1.575	1.578	197	198
PAA	1.497	-	-	−
PDMS	1.404	-	-	-

[a] Uncertainty is 1 σ of the pooled variance of duplicate measurements for each blend.

uncertainties in index and thickness are one standard deviation based on the pooled variance of duplicate measurements.

Optical Microscopy (OM). The wrinkled surface was imaged by an optical microscope (Nikon, Optiphot-2) to measure the wavelength using 20×, 50×, and 100× objectives. The wavelength was extracted either by converting the real space images into Fourier space or the wavelength was measured by averaging at least 8 values from different calibrated images along the film surface area. The images were treated with ImageJ (Rasband, W. S., ImageJ, NIH: Bethesda, MD, http://rsb.info.nih.gov/ij/, 1997−2008) and converted to Fourier space via the application of fast Fourier transform algorithms (FFT) to get the dominant wave vector $q_m\,\mu m^{-1}$ followed by conversion to wavelength by applying the relationship $d_m = 2\pi/q_m$. Both procedures yielded nearly identical results. All reported standard uncertainty in wrinkles wavelength is one standard deviation based on the pooled variance of at least 12 measurements.

Atomic Force Microscopy (AFM). Surface analysis of the annealed films was performed in tapping mode using a Nanoscope IV (Digital Instruments) with phosphorus doped silicon tips. Root mean square (rms) roughness data was collected from each sample using standard methods. Multiple 5 μm × 5 μm regions were scanned for each sample and were used to measure the wrinkling wavelength. All reported standard uncertainties in roughness are one standard deviation based on the pooled variance of at least 5 measurements.

Results

In this work, the elastic moduli of the p(DTE carbonate), p(I_2-DTE carbonate) and 75:25, 50:50, 25:75, 10:90% by mass discrete blends were measured using either uniform or gradient thickness approaches. The homopolymers are amorphous, glassy poly(amide-carbonate) systems with glass transition temperatures, T_g, of 100 and 145 °C respectively. The discrete blends of the two polymers are homogeneous mixtures on the microscale as revealed from atomic force microscopy (AFM). X-ray photoelectron spectroscopy (XPS) (see Supporting Information) further confirmed the as mixed composition of the materials were present on the surface of the annealed polymer films. The homogeneity is pertinent to our study since the elastic modulus represents the entire sample and is not function of an individual component or phase.

The phase behavior of the blend was explored further using dynamic mechanical analysis (DMA). Data were collected for p(DTE carbonate), p(I_2-DTE carbonate), and their 50:50 by mass blend at 1 Hz frequency in the tension mode as a function of temperature (−150 °C to T_g + 10 °C), Figure 1. The DMA spectra have in general secondary relaxations in the T range −150 to −50 °C that is separated from the α relaxation (T_g) that shows up at 100 °C for p(DTE carbonate) and 145 °C for p(I_2 DTE carbonate). The two distinct α-relaxation processes, present in the DMA measurement of the 50:50 blend, suggest the material is phase-separated on a fine scale. The two materials seem to be partially miscible which is why large scale phase separation was not observed in the AFM images. Also present in the spectra are the composition dependent broad β-relaxations of the tyrosine derived polycarbonates p(DTR carbonate), where R denotes an alkyl substituent in the ester position. The relaxation behavior of p(DTR carbonates) is well-documented and the molecular relaxation mechanisms of the tyrosine-derived polycarbonates were investigated previously by measuring thermally stimulated depolarization currents (TSDC) as a function of temperature.[28−32] These relaxation mechanisms contribute significantly to the mechanical properties of polycarbonates especially in the thin film regime where the polymer chains exhibit strong intersegment interactions coupled with secondary relaxation behavior. The implication of the relaxation behavior will be described further in the discussion section.

The thin films were prepared using a flow coating method[27] on top of Si wafers precoated with a PAA release layer to facilitate relatively defect and stress free film transfer from Si to PDMS for subsequent wrinkling. We were unsuccessful in transferring films from either oxidized Si wafers or hydrophobic (alkane silyanization) substrates. While this approach was successful, the use of a release layer to facilitate film transfer increased the roughness of the exposed interface. We found the p(DTR carbonate) surface roughness to correlate with the thickness of the PAA release layer; thinner PAA release layers reduced the resulting surface roughness. The roughening is attributed to the formation of an intermixed layer that results during the flow coating process and presents itself when the PAA layer is removed. While we have taken great care to accurately measure the magnitude of the surface roughness in the thickness measurements, the full impact of surface roughness on the thin film modulus will be the subject of a separate study. We were careful to consider the influence of uncertainty in our thickness calculations and chose to stop our reported modulus values at 30 nm. We could not reproducible transfer films below this thickness value which were defect free and where the rms roughness did not exceed 25% of the targeted thickness value. The overall film preparation and the transfer onto PDMS with subsequent wrinkling steps are shown schematically in Figure 2b.

When applying eq 2 to measure the modulus of thin polymer films, precise measurements of both the wavelength of the wrinkles and the film thickness is essential since the elastic modulus, E_f, varies with the third power of their ratio. Variable angle spectroscopic ellipsometry (VASE) data modeling was used to characterize the film thickness of both pre- and post-transferred films. Shown in Figure 3 are VASE data and the model fits for a p(DTE carbonate) homopolymer film where the PAA thickness was fixed at the value independently measured prior to coating of ≈ 63 nm. For films on the PAA release layer, a five phase model was used (Si, native oxide, PAA, film, air) to analyze the data, as shown in the inset to Figure 3a. In Figure 3a, only the thickness and refractive index of the p(DTE carbonate) was varied. As can be seen, the model fit is poor. By allowing the underlying PAA thickness to adjust (Figure 3b) the fit is clearly superior indicating that a significant amount of PAA was dissolved or swept aside during the flow coating process. Typical PAA model film thicknesses after flow coating were 0 to 10 nm. The modeling was generally improved by inclusion of ≈ 5% nonuniformity (incoherent superposition of multiple models) in the blend film thickness, consistent with slight visible variations in the film thickness. Shown in Figure 3d is the derived dielectric function for the homopolymers: p(DTE carbonate) and p(I_2-DTE carbonate) and the PAA release layer.

After transfer to the PDMS, the blend films were again measured and modeled by a four phase model (air, PDMS, film,

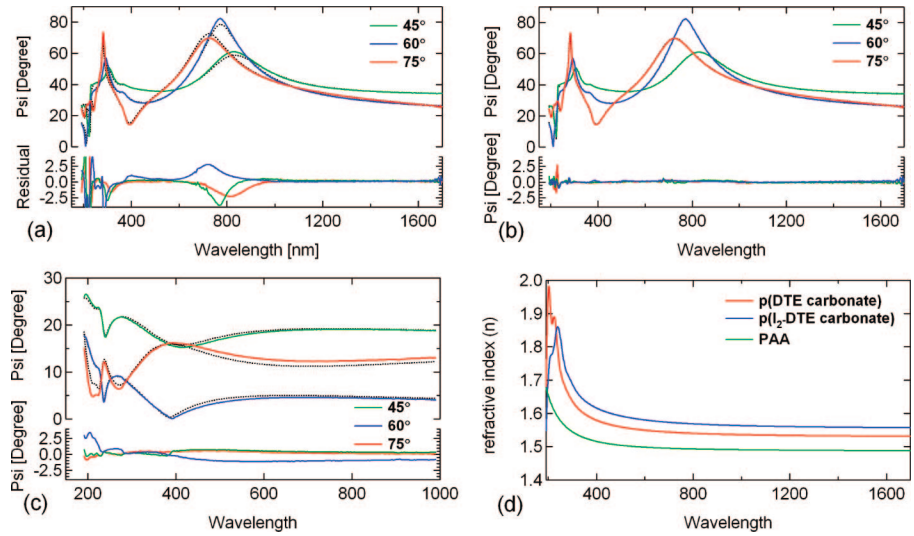

Figure 3. VASE data (ellipsometric parameter psi) and the respective fits (black line) to each model. a) Assumes initial PAA layer (63 nm) is fully retained during flow coating. Best fit p(DTE carbonate) film thickness is 88 nm. b) Assumes initial PAA layer is partially swept away during flow coating. Best fit p(DTE carbonate) thickness is 140 nm; residual PAA layer thickness is 9 nm. c) VASE data and model fits for p(DTE carbonate) film transferred to stretched PDMS with best fit film thickness of 144 nm and surface roughness of 4 nm. d) Derived refractive index for p(DTE carbonate), p(I_2-DTE carbonate) and PAA.

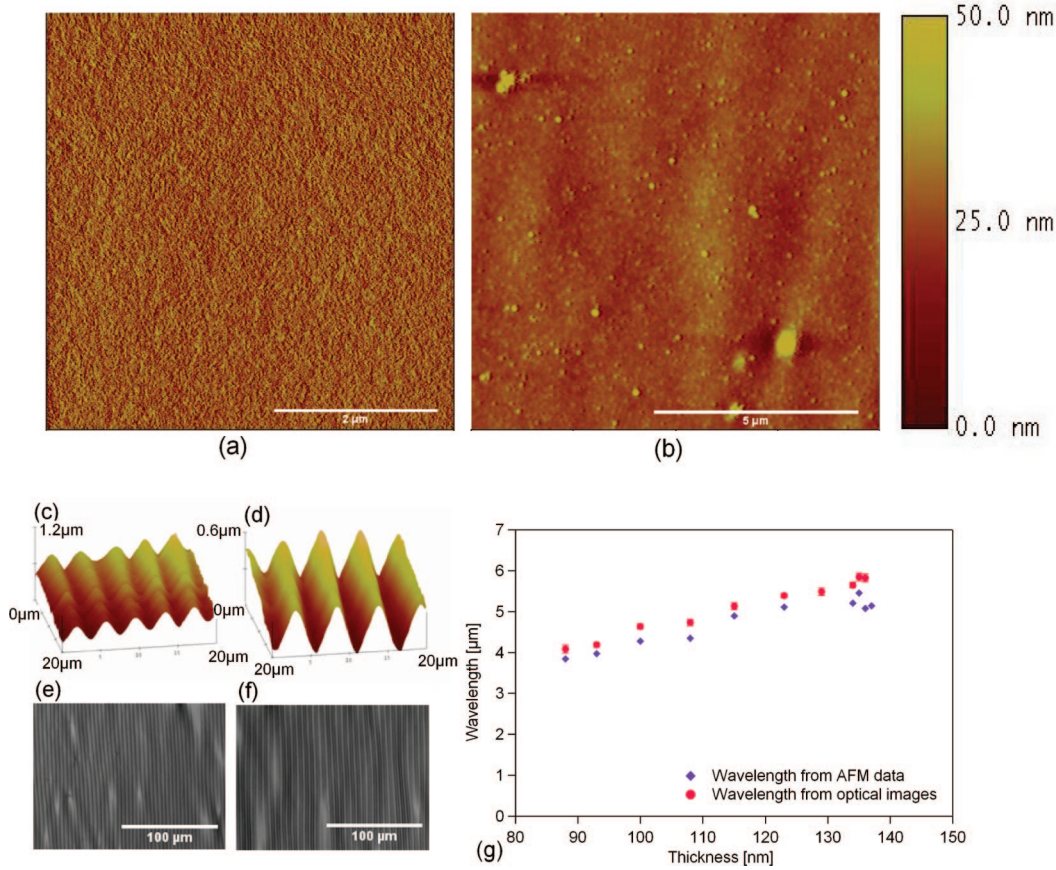

Figure 4. AFM and optical images of the periodic wrinkles generated during the wrinkling process of the p(DTE carbonate) gradient thickness film. Key: (a and b) AFM height image of p(DTE carbonate) pre- and post-transferred films (rms roughness 0.27 ± 0.1 nm and 7.50 ± 3.2 nm respectively), (c and d) AFM 3D images corresponding to films of 88 and 135 nm thickness, respectively, and (e and f) the corresponding optical images for the area containing AFM spots in the gradient thickness film. (g) Plot shows the wrinkle wavelength for the p(DTE carbonate) film as a function of thickness obtained from AFM (open circles) and optical images (closed circles).

air). The dielectric constant derived from the pretransfer measurements was used for the film. It was necessary to include a correction for the reflection from the back surface of the PDMS film (modeled by an incoherent superposition of signals). The presence of the back interface in general degraded the ability to model the data, presumably due to partial coherence in the experiment. Shown in Figure 3c is the VASE data and model fit for the film reported in Figure 3, parts a and b. The transferred film thickness was measured to be in good agreement with the pretransfer film thickness. The ratio of post- to pre- transfer

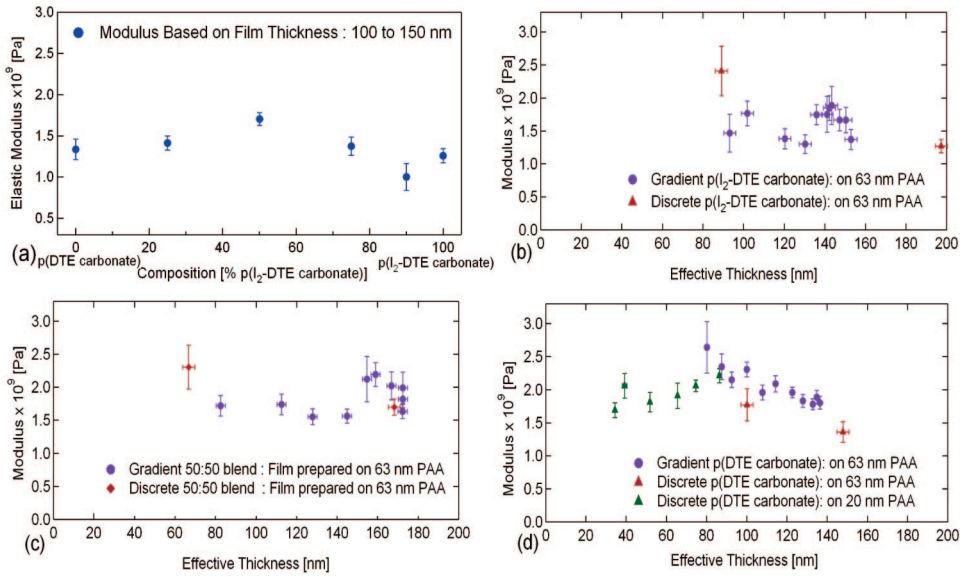

Figure 5. Elastic moduli of the respective polymer films. (a) Modulus as a function of composition for films 100−150 nm in thickness. (b−d) Modulus of p(I_2-DTE carbonate), 50:50 blend and p(DTE carbonate) films as a function of thickness based on post-transfer film thicknesses to PDMS. Modulus error bars is ±1 unit standard deviation. Thickness error is ±2 nm.

thickness is 0.96 ± 0.06. A significant source of the uncertainty in this ratio is the correlation between residual PAA thickness and blend thickness. Attempts were made to determine the sensitivity of the VASE measurements to the presence of a residual PAA layer on the top of the transferred films. Slight improvement in the fit quality was obtained by inclusion of a 1 to 2 nm top PAA layer. Alternatively, inclusion of 2 to 3 nm of surface roughness (modeled as a 50% Bruggeman effective medium approximation, EMA, of film and void) always produced better fits than the inclusion of residual PAA. Combining the comparison of transferred film thickness with these results indicate that there is no significant, greater than a few nanometers, residual PAA. For the gradient film studies, only transferred film thicknesses were measured and modeled relying on the models developed for the uniform thickness films.

The wrinkle wavelength, *d*, was ascertained by treating optical images of the wrinkled surfaces in real space or in Fourier space to extract the periodicity of the wrinkling pattern as discussed in the experimental section. This ensured that the obtained value of *d* was consistent and representative of the probed spot. The measurements were confirmed via AFM for the p(DTE carbonate) gradient film of the same surface at the approximate same locations as shown in Figure 4g.

Blend Composition Studies. The elastic modulus of p(DTE carbonate), p(I_2-DTE carbonate) homopolymers and their discrete composition blends (25:75, 50:50, 75:25, and 10:90% by mass) were measured using uniform films with thickness in the range 150 to 200 nm. Following film transfer and thorough characterization of film thicknesses, the respective films were subjected to a compressive strain, a maximum of 1.5%. The resulting wrinkles were of sinusoidal shape and covered the entire film surface. Shown in Figure 5a are the moduli, calculated *via* eq 2 as a function of polymer composition for the p(DTE carbonate), p(I_2-DTE carbonate) and their blends for the two discrete thickness ranges using the post-transfer film thicknesses. In the calculation, the Poisson's ratio for P(DTR carbonate) and PDMS was taken to be 0.33 and 0.5, respectively. The PDMS modulus was determined by tensile test. The modulus data uncertainty is reported in terms of one standard deviation of the data variation. The subtle variations arise from films of slightly different thickness. In general, the modulus exhibits no significant trend with increasing p(I_2-DTE carbonate) content in the blends.

Variation of Modulus with Thickness. In order to evaluate the effect of progressively reducing film thickness on the measured modulus, gradient thin films of p(DTE carbonate), p(I_2-DTE carbonate), and their 50:50 blend were subjected to controlled wrinkling instabilities in the global range from 85 to 172 nm. The specific ranges and the resulting moduli are depicted in Figure 5. Parts b−d of Figure 5 show the compiled modulus as a function of film thicknesses based on post-transferred film thickness for the three gradient films. The p(DTE carbonate) moduli data of the gradient sample exhibit a small decrease of 10%−12% in the modulus as the thickness increases above 100 nm.

Neglecting any variation in thickness, the combined data in parts b−d of Figure 5 provide a more stringent assessment of the composition dependence of the modulus. Comparing the moduli of the three gradient films grouped over their entire thickness ranges by one factor three levels ANOVA show that there are small statistical differences at a 95% confidence between the moduli mean in agreement with very weak dependence to of the moduli on composition in the order p(DTE carbonate) > 50:50 > p(I_2-DTE carbonate). The total decrease across the series is ≈20%, too weak to be clear in Figure 5a.

The gradient thickness approach was supplemented by a series of discrete p(DTE carbonate) film thickness in the thickness range 80 to 30 nm. This approach was implemented to reduce the uncertainty associated with the thickness measurement in the gradient films arising from the variation across the VASE spot, 3 mm. Shown in Figure 5d are the modulus data for the p(DTE carbonate) from 80 to 30 nm in the same graph containing the gradient data. The discrete and gradient data agree well; a comparison of the discrete thickness data between 80 to 30 nm and the gradient thickness data between 136 to 80 nm by one factor two levels, ANOVA, indicates no statistical differences between their means. Challenges associated with maintaining film integrity during film transfer prevented further probing below 30 nm.

Discussion

While facilitating relatively stress free film, the use of the PAA release layer presents challenges related to accurate assessment of film thickness. As we implied earlier, the secondary flow coating process leads to the creation of an interfacial mixed layer which subsequently generates a rougher

air-polymer surface. In order to understand this process, characterization of the double layer is mandated. Our model system involves two thin films sequentially laid down on the Si substrate. From the VASE measurements, the PAA layer thickness was reduced during the flow coating of the top p(DTR carbonate) layer possibly due to gravitational forces inherent to the flow coating method. The change in PAA layer thickness is associated with the creation of an interfacial mixed layer between PAA and p(DTR carbonate) layers attributed to trace water dissolution of PAA in the p(DTR carbonate) solution. This interfacial layer is probably a mix of the two polymer layers which upon removal of PAA by water will leave a rough p(DTR carbonate) layer with a rough surface. This rough surface is crucial to the thin film modulus measurements since the contribution of the surface roughness to the film thickness increases with the reduction of film thickness. The interfacial layer surface was characterized post-transfer to the PDMS after excessive washing of PAA by both AFM and VASE measurements. AFM height images showed that the rms roughness of the p(DTE carbonate) film surface generated from the double layer with 63 nm PAA thickness to be in order of 7.5 ± 3.2 nm and it is an order of magnitude larger than the rms roughness 0.3 ± 0.1 nm of a flow coated p(DTE carbonate) films on Si substrate, Figure 4, parts a and b. The VASE measurements were performed on the PAA−p(DTE carbonate) double layer on Si substrate and on p(DTE carbonate) film after being transferred onto prestretched PDMS substrate. For the double layer, no statistically significant improvement in the VASE modeling was obtained by including either surface roughness or an effective medium interlayer between the PAA and p(DTE carbonate) layer. Despite the inability of the VASE model to capture the interfacial mixed layer, the overall reduction in the PAA layer thickness upon flow coating p(DTE carbonate) layer was clear. For the p(DTE carbonate) film on prestretched PDMS, the VASE model showed that inclusion of surface roughness of 2−3 nm (modeled by Bruggeman EMA, with 50% void) always produced better fits than inclusion of PAA residues. The modeled VASE measurements also indicated that using a thick PAA layer is more likely to produce a rough p(DTE carbonate) surface after the transfer process due to the dissolution of more PAA. This result has led us to reduce the PAA release layer thickness from 63 to 20 nm when preparing the discrete p(DTE carbonate) film within 30 to 80 nm thickness in order to mitigate the effect of generated surface roughness. In addition, because of the correlations between the estimated PAA residual layer and the p(DTR carbonate) overlayer, all reported modulus data is based on post-transfer p(DTR carbonate) film thicknesses. This is an important consideration for others performing similar experiments using sacrificial release layers.

Thin film elastic modulus, E_f, is one of the fundamental polymer properties that is thought to change as a function of film thickness.[33−35] Factors that influence and determine these changes include the interfacial interactions of the relative monomer−monomer, and monomer-interface (substrate or free surface). The impact of confinement on material properties is pertinent to the glassy state dynamics and the associated relaxation behavior.[34] For the p(DTE carbonate), the moduli reported within 30 to 80 nm thickness range from the discrete samples with thin PAA release layers, minimized roughness, most stringently tests the influence of surface confinement. According to eq 1, the linear relationship where $d \sim h_f$ holds and a plot of wrinkle wavelength vs film thickness should have a zero intercept. A finite intercept has been described previously as evidence for a thin, confinement altered, layer.[22] Shown in Figure 6 is the p(DTE carbonate) data along with the best linear fit and the 95% confidence bands. The wavelength of the wrinkles can be fit linearly with the film thickness over the experimental range which yields a small offset of 2.7 nm that is not significant at the 95% level. For other materials, the effect of confinement on the polymer thin film mechanics has been reported previously for polystyrene, PS, and polyvinyl acetate, PVAc.[36−38] Employing the microbubble inflation technique, the biaxial creep compliance of free-standing ultrathin films was determined. Both PS and PVAc showed dramatic stiffening in the rubbery plateau below 100 nm thickness. In recent work, McKenna reported that PS free-standing thin films to show 2.5 times (250%) stiffening in the glassy regime relative to the bulk within the linear viscoelastic regime based on biaxial compliance data for films between 11.3 to 112 nm thickness.[36]

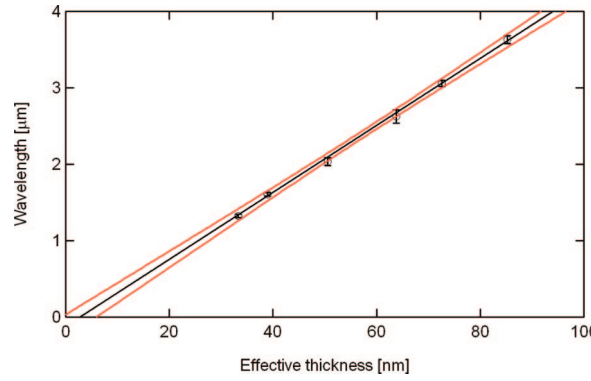

Figure 6. Wavelength of the wrinkles as a function of film thickness from the p(DTE carbonate) discrete film thickness series. Solid line represents best fit of data (black) and the 95% confidence bands (red).

Conclusions

In summary, the elastic moduli of p(DTE carbonate), p(I_2-DTE carbonate) homopolymers and their blends as a function of composition and film thickness are reported. Gradient and discrete film thickness approaches were employed to measure the elastic modulus of thin films over a 30 to 200 nm thickness range which is an important range for coatings and delivery systems in biomedical applications. The elastic modulus was found to be weakly dependent on composition as the % mass of p(I_2-DTE carbonate) in the blend increases. Similarly, the impact of film thickness on modulus of p(I_2-DTE carbonate), and their 50:50 by mass blend shows very weak to null effect. While the measured elastic moduli of p(DTE carbonate) increased slightly 10−15% below 100 nm, we were unable to reliably transfer films below 30 nm in thickness where any significant deviations from the measured modulus values have occurred in other reports. This work highlights the substantial challenges with accurately quoting a thickness following film transfer using a release layer. Furthermore it calls into question the influence of roughness and defect contributions to thickness assessments and the associated mechanical properties. These are topics that require more a focused analysis in the future.

Acknowledgment. The authors thank Dr. Christopher Soles and Dr. Jack F. Douglas from NIST and Professor Alexei Sokolov from the University of Akron for useful discussions during the course of this work. The polymers were synthesized at the New Jersey Center for Biomaterials supported by "RESBIO"—the Integrated Resource for Polymeric Biomaterials (NIH Grant P41 EB001046).

Supporting Information Available: A figure showing the normalized XPS iodine peaks. This material is available free of charge via the Internet at http://pubs.acs.org.

References and Notes

(1) Pulapura, S.; Kohn, J. *Biopolymers* **1992**, *32*, 411–417.
(2) Meechaisue, C.; Dubin, R.; Supaphol, P.; Hoven, V. P.; Kohn, J. *J. Biomater. Sci.-Polym. Ed.* **2006**, *17*, 1039–1056.

(3) Kohn, J.; Zeltinger, J. *Exp. Rev. Med. Dev.* **2005**, *2*, 667–671.
(4) Bourke, S. L.; Kohn, J. *Adv. Drug Delivery Rev.* **2003**, *55*, 447–466.
(5) Hoven, V. P.; Poopattanapong, A.; Kohn, J. *Macromol. Symp.* **2004**, *216*, 87–97.
(6) Sharma, R. I.; Kohn, J.; Moghe, P. V. *J. Biomed. Mater. Res. Part A* **2004**, *69A* (1), 114–123.
(7) *AIGISRX Anti-Bacterial Envelope*; 510(k): k063091; Food and Drug Administration: 510(k): k063091, Jan. 16, **2008**.
(8) Bailey, L. O.; Becker, M. L.; Stephens, J. S.; Gallant, N. D.; Mahoney, C. M.; Washburn, N. R.; Rege, A.; Kohn, J.; Amis, E. J. *J. Biomed. Mater. Res. Part A* **2006**, *76A*, 491–502.
(9) Bourke, S. L.; Kohn, J.; Dunn, M. G. *Tissue Eng.* **2004**, *10* (1−2), 43–52.
(10) Liu, E.; Treiser, M. D.; Johnson, P. A.; Patel, P.; Rege, A.; Kohn, J.; Moghe, P. V. *J. Biomed. Mater. Res. Part B* **2007**, *82B* (2), 284–297.
(11) Sheihet, L.; Dubin, R. A.; Devore, D.; Kohn, J. *Biomacromolecules* **2005**, *6*, 2726–2731.
(12) Jay, M. J.; Ryo, U. Y. Biodegradable low biological toxicity radiographic contrast medium and method of x-ray imaging. 5019370, **1991**.
(13) Kohn JB, B. D., Pendharkar S. M. Radio-opaque polymer biomaterials. 7056493, **2006**.
(14) Yang, Y. Y.; Dorsey, S. M.; Becker, M. L.; Lin-Gibson, S.; Schumacher, G. E.; Flaim, G. A.; Kohn, J.; Simon, C. G. *Biomaterials* **2008**, *29*, 1901–1911.
(15) Macario, D. K.; Entersz, I.; Bolikal, D.; Kohn, J.; Nackman, G. B. *J. Biomed. Mater. Res. Part B: Appl. Biomater.* **2008**, *86B* (1), 237–244.
(16) Zhao, J. H.; Kiene, M.; Hu, C.; Ho, P. S. *Appl. Phys. Lett.* **2000**, *77*, 2843–2845.
(17) Stafford, C. M.; Vogt, B. D.; Harrison, C.; Julthongpiput, D.; Huang, R. *Macromolecules* **2006**, *39*, 5095–5099.
(18) Bohme, T. R.; de Pablo, J. J. *J. Chem. Phys.* **2002**, *116*, 9939–9951.
(19) Van Workum, K.; de Pablo, J. J. *Nano Letters* **2003**, *3*, 1405–1410.
(20) Yoshimoto, K.; Jain, T. S.; Nealey, P. F.; de Pablo, J. J. *J. Chem. Phys.* **2005**, *122* (14), 6.
(21) Stoykovich, M. P.; Yoshimoto, K.; Nealey, P. F. *Appl. Phys. A-Mater. Sci. Process.* **2008**, *90* (2), 277–283.
(22) Stafford, C. M.; Harrison, C.; Beers, K. L.; Karim, A.; Amis, E. J.; Vanlandingham, M. R.; Kim, H. C.; Volksen, W.; Miller, R. D.; Simonyi, E. E. *Nat. Mater.* **2004**, *3* (8), 545–550.
(23) Huang, J.; Juszkiewicz, M.; de Jeu, W. H.; Cerda, E.; Emrick, T.; Menon, N.; Russell, T. P. *Science* **2007**, *317* (5838), 650–653.
(24) Wilder, E. A.; Guo, S.; Lin-Gibson, S.; Fasolka, M. J.; Stafford, C. M. *Macromolecules* **2006**, *39*, 4138–4143.
(25) Mei, H. X.; Huang, R.; Chung, J. Y.; Stafford, C. M.; Yu, H. H. *Appl. Phys. Lett.* **2007**, *90*−1−3.
(26) Fiordeliso, J.; Bron, S.; Kohn, J. *J. Biomater. Sci., Polym. Ed.* **1994**, *5*, 497–510.
(27) Stafford, C. M.; Roskov, K. E.; Epps, T. H.; Fasolka, M. J. *Rev. Sci. Instrum.* **2006**, *77* (2), 023908.
(28) Suarez, N.; Laredo, E.; Bello, A.; Kohn, J. *J. Appl. Polym. Sci.* **1997**, *63*, 1457–1466.
(29) Suarez, N.; Brocchini, S.; Kohn, J. *Polymer* **2001**, *42*, 8671–8680.
(30) Puma, M.; Suarez, N.; Kohn, J. *J. Polym. Sci., Part B: Polym. Phys.* **1999**, *37*, 3504–3511.
(31) Suarez, N.; Brocchini, S.; Kohn, J. *Radiat. Eff. Defects Solids* **2001**, *155* (1−4), 379–385.
(32) Tangpasuthadol, V.; Shefer, A.; Yu, C.; Zhou, J.; Kohn, J. *J. Appl. Polym. Sci.* **1997**, *63*, 1441–1448.
(33) Forrest, J. A.; Dalnoki-Veress, K. *Adv. Colloid Interface Sci.* **2001**, *94*, 167–196.
(34) Pharm, J. Q.; Green, P. F. *J. Chem. Phys.* **2002**, *116*, 5801–5806.
(35) Zhao, J.-H.; Kiene, M.; Hu, C.; Ho, P. S. *Appl. Phys. Lett.* **2000**, *77*, 2843–2845.
(36) O'Connel, P. A.; Hutcheson, S. A.; McKenna, G. B. *J. Polym. Sci., Part B: Polym. Phys.* **2008**, *46*, 1952–1956.
(37) O'Connell, P. A.; McKenna, G. B. *Science* **2005**, *307* (5716), 1760–1763.
(38) O'Connell, P. A.; McKenna, G. B. *Eur. Phys. J. E* **2006**, *20* (2), 143–150.

MA802115B